# Molecular Dynamics Simulations of Precursor Ceramic with Sil-Ma Composite

## Xintong Shi, Xujing Zhang\*, Wenbo Zhu, Zhitao Yin

College of Mechanical Engineering, Xinjiang University, Urumqi 830046, Xinjiang Uygur Autonomous Region, China \*Correspondence to: zzbutterfly@foxmail.com

#### Abstract

Molecular dynamics (MD) simulations were used to investigate the interfacial interactions of hydroxyapatite,  $\beta$  tricalcium phosphate, sil-ma, and filin protein (SF) in the composite. This study analyzed the interface binding energy and radial distribution function between hydroxyapatite (HA),  $\beta$  triccalcium phosphate ( $\beta$ -tcp), sil-ma and bio-polymer SF. The study found that the interface binding energy of Sil-MA hybrid system is higher than that of SF hybrid system, indicating that the Sil-MA hybrid system is more stable, which makes the mechanical properties of this system better.

Keywords: sil-ma; Molecular dynamics; Precursor ceramic

#### Introduction

Hydrogels are water-containing materials with good biocompatibility, biodegradability and other special functions, which have been applied in many fields such as tissue engineering, drug sustained-release, disease treatment and so on. As soft materials, hydrogels have attracted much attention in the field of cartilage repair. Sil-MA hydrogel obtained by modifying fibroin protein (SF) with glycidyl methacrylate (GMA) has also been used by more and more researchers to repair cartilage damage. Sil-MA hydrogel has more stable physical and chemical properties, high elastic modulus, and is a good carrier for cells [1]. Its biocompatibility and biodegradability make it very useful in cartilage repair applications.

For Sil-MA hydrogel as a material modified by SF, the content of GMA in the hydrogel directly affects its properties. Son <sup>[2]</sup> et al. evaluated the effect of different contents of GMA on the mechanical properties of Sil-MA, and added 424 mM Sil-MA showed excellent mechanical properties. According to the study of its mechanical properties, the mechanical properties of Sil-MA hydrogel increase with increasing concentration, and the compressive stress of Sil-MA hydrogel is up to 910 kpa at 30% and can be restored after compression. In the cartilage treatment study, Wu <sup>[3]</sup> et al. used Sil-MA hydrogel as biological glue to enhance the lateral integration of bone scaffold with the host, and found that the high viscosity of Sil-MA hydrogel made it free from bleeding around the gap after filling the gap of the stent.

However, because the mechanical properties of hydrogel cannot meet the treatment of cartilage damage, other materials need to be added to improve the mechanical properties. The hydroxyapatite (HA) is used as the main material of bone implants due to its good bone induction characteristics and bone conductivity, and its high biocompatibility and the ability to integrate  $^{[4]}$  with natural bone tissue, which has been widely used in basic research and clinical aspects. However, its poor bending strength and great fragility limit its application in implants. Many scholars have improved the defects of HA through the form of composite materials.  $\beta$  -TCP has a fast dissolution rate, which gives it good biodegradability, but the rapid dissolution will reduce the mechanical strength of the scaffold  $^{[5]}$ . However, HA has higher mechanical strength and lower degradation rate than  $\beta$  -TCP, so the researchers studied HA /  $\beta$  -TCP composite scaffold and proved that HA /  $\beta$  -TCP composite can combine the advantages of the two and improve the physical, chemical, mechanical and biological properties  $^{[6]}$ . Liu  $^{[7]}$  et al prepared a biomimetic multi-layer bone-cartilage scaffold by adding HA, which improved the mechanical properties of the hydrogel by changing the HA content in the study. The sil-ma used in this study has stable physicochemical properties and good biocompatibility, but there are problems of poor mechanical properties and fast degradation rate, and combining these materials can compensate for the poor mechanical properties of the hydrogel, improve the mechanical properties of the hydrogel, and improve the degradation cycle of the gel.

Many researchers have extensively studied the macroscopic mechanical behavior of tissue engineered materials while their physical and mechanical properties of HA,  $\beta$  -tcp and polymer materials are influenced not only by HA particle size and volume fraction but also by the interfacial adhesion between HA,  $\beta$  -tcp packing and polymer materials [8]. Therefore, in order to study and analyze the mechanical properties of SF and Sil-MA, it is also very important to study the influence of intermaterial bonding and interface binding energy on the mechanical properties of mixed materials at the molecular level. Molecular dynamics (MD) simulation technology has been developed into a powerful scientific tool for building, displaying

Vol: 2025 | Iss: 1 | 2025 | © 2025 Fuel Cells Bulletin

and analyzing structural models of molecules, solids and surfaces to study their properties. Combining micromechanical and macroscopic experimental data from molecular dynamics simulations, the properties of the material can provide a more comprehensive scientific interpretation of [9][10][11].

Sun et al.  $^{[12]}$ , using molecular dynamics simulations to study different water content. Effect on the network structure and oxygen permeability of polygel (double (trimethyl siloxyl) methylsilylglycerol methacrylate (PSiMA) and poly (2-methylacrylooxynyl phosphocholine) (PMPC) hydrogels. The results show that the increase in water content of the hydrogel is closely associated with its decrease in oxygen permeability. Tan et al.  $^{[13]}$  can successfully explore how charged amino acid residues lead to HA NPs nucleation through MD simulation studies. In this study, MD simulation was used to study the interface binding energy of HA and  $\beta$  -tcp crystal surfaces and two polymer materials, and analyze the radial distribution function and binding energy and obtain the influence of the interface binding energy on the mechanical properties. It provides a microscopic theory basis for the macroscopic mechanical behavior of hybrid materials.

### Molecular dynamics studies

Firstly, the theoretical analysis of the experimental materials is conducted for HA,  $\beta$  -tcp, SF and Sil-ma. Because Sil-ma is Sil-ma hydrogel after photocuring, which is the self-assembly behavior of the photoinitiator Sil-ma hydrogel, the Sil-ma model construction, and the molecular dynamics simulation after the model construction.

#### 2.1 Model construction

The space group of HA is P21 / b and its lattice parameters a = b = 9.432 Å and c = 6.881 Å  $^{[14,15]}$ . In HA crystals, OH ions form arrays in a direction parallel to the c axis; each OH ion is coordinated with three Ca atoms that form tritriangle in the same plane. Looking along the c-axis, each of the two adjacent Ca atoms can be matched together after  $60^{\circ}$  of rotation, located in two different planes. All force field parameters of the atoms in HA are assigned under the Dreiding force field and assigned to the atoms in HA: Ca + 2.0, P + 2.6, H + 0.6, and O-1.44 and-1.6 indicate O in OH. The HA crystal surface was cut along the  $(0\ 0\ 1)$ ,  $(1\ 0\ 0)$  and  $(1\ 1\ 0)$  planes and then minimized under periodic boundary conditions with a non-bond cut-off distance of 9.5 Å . The minimization process includes the steepest descent method 1 Å that converges to 1000 kcal / mol<sup>-1</sup>, Which was followed by a conjugate gradient of 1 Å that converged to  $10\ \text{kcal}$  / mol<sup>-1</sup>, Finally finally the BFGS algorithm 1 Å with convergence of  $0.1\ \text{kcal}$  / mol<sup>-1</sup>, see Figure 1-3.

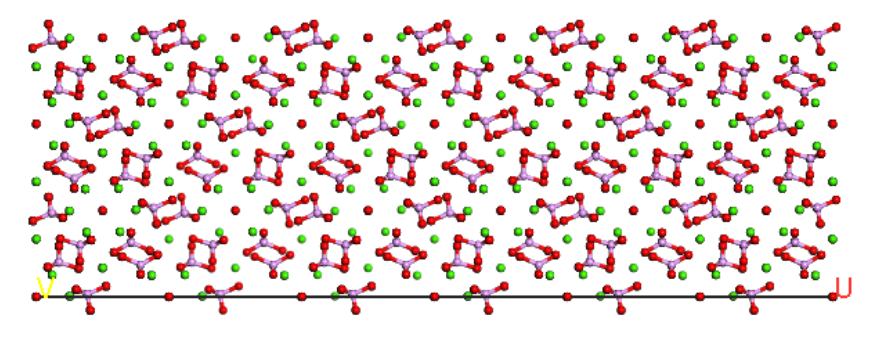


Figure 1 100 for the surface

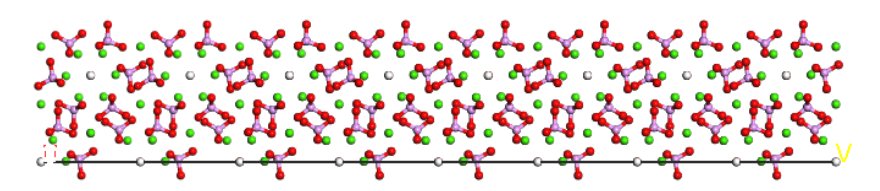


Figure 2 110 for the surface

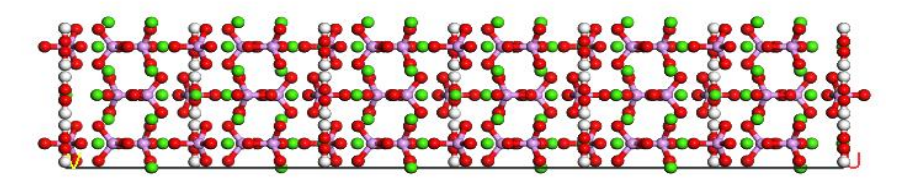


Figure 3 001 for Surface

Figure 1,2, and 3 shows the surface ball-and-stick model of HA. Figure 1:100, Figure 2:110, and Figure 3:001. Color represents: calcium atoms (green), hydrogen atoms (white), oxygen atoms (red), phosphorus atoms (purple).

The  $\beta$ -tcp whose space group is 1 P1 and its lattice parameters are a = b = 10.5492A, c = 37.6776~A. In the  $\beta$ -tcp crystal, three calcium ions are coordinated to each phosphate ion. All force field parameters of the atoms in B -tcp are assigned under the Dreiding force field, and the  $\beta$ -tcp crystal surfaces are cut along (0 0 1), (1 0 0) and (1 1 0) planes and then minimized under periodic boundary conditions with a non-bond cutoff distance of 9.5 A.as shown in the figure 4-6:

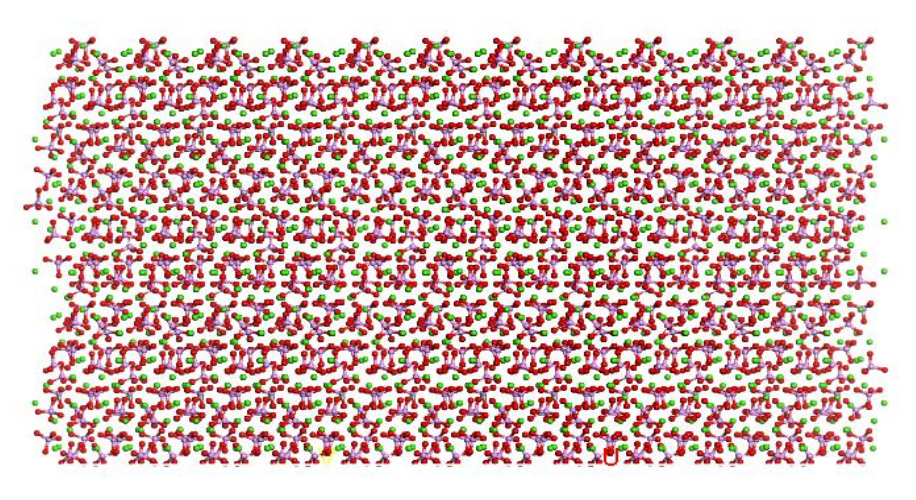


Figure 4 001 Surface model

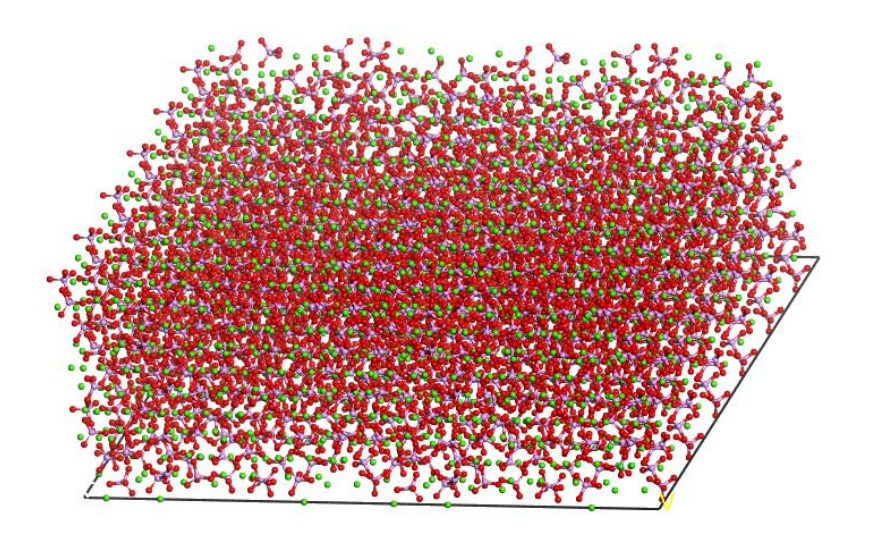


Figure 5 100 for the surface model

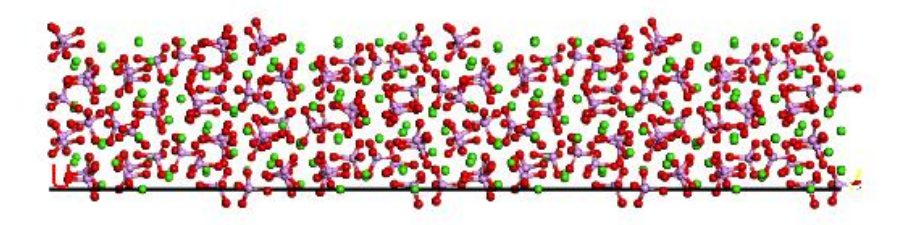


Figure 6 110 surface model

Figure 4,5 and 6 show the surface-ball-stick model of  $\beta$  -TCP. Figure 4:001, Figure 5:100, and Figure 6:110. Color represents:

calcium atoms (green), oxygen atoms (red), phosphorus (purple).

The SF molecular chain is a structure constructed and optimized by using a protein model using the MD calculation under the chimera software to obtain a stable configuration of 300ps under the NVE ensemble 50K parameter.sil-ma hydrogel obtained by GMA methacryloylation SF has more stable physical and chemical properties, high elastic modulus is a good carrier of cells, and adding LAP light initiator can be applied to DLP printed light curing hydrogel, the formation principle is on SF molecules by GMA modification, epoxy group of GMA molecule ring [16], while alcohol for CHOH stretching behavior, under the action of light cross-linking agent LAP, self-assembly behavior formed light curing sil-ma, see Figure 7-10.

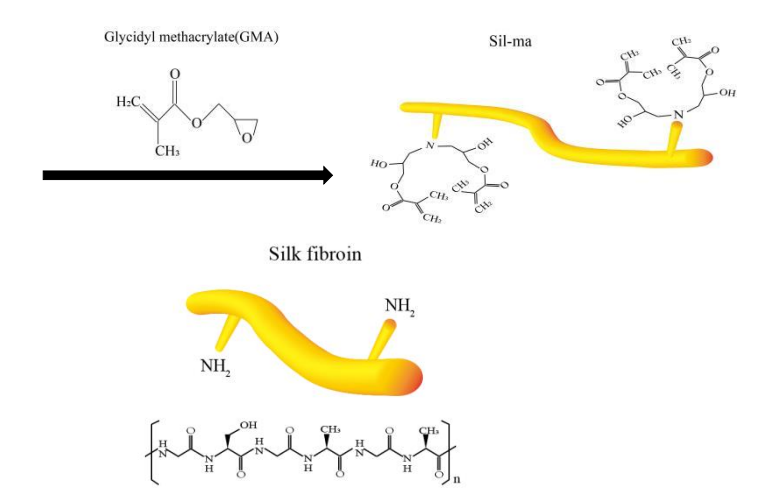


Figure 7 Preparation principle of Sil-MA

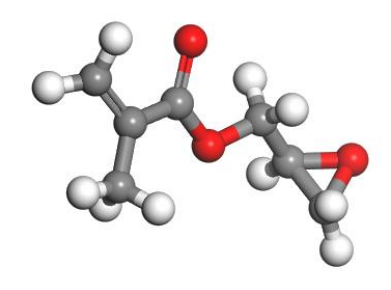


Figure 8 The molecular structure of GMA

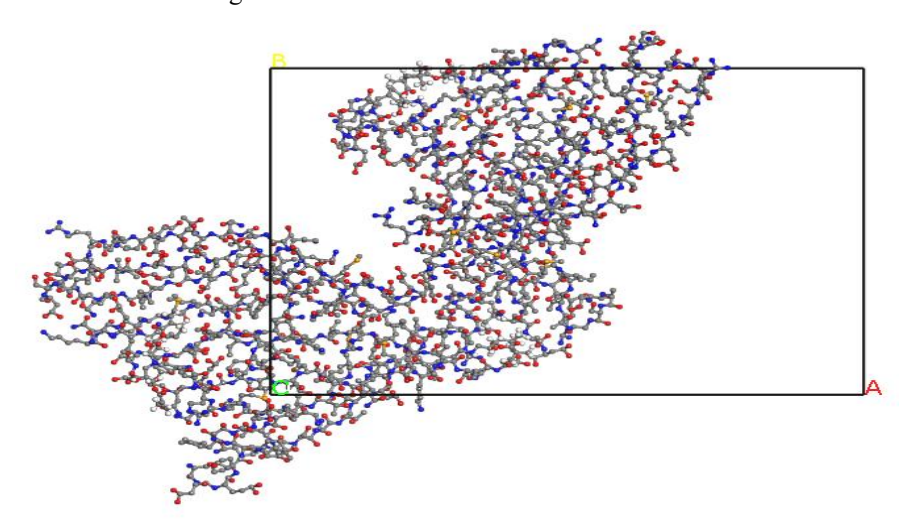


Figure 9 Structural model of Sil-MA

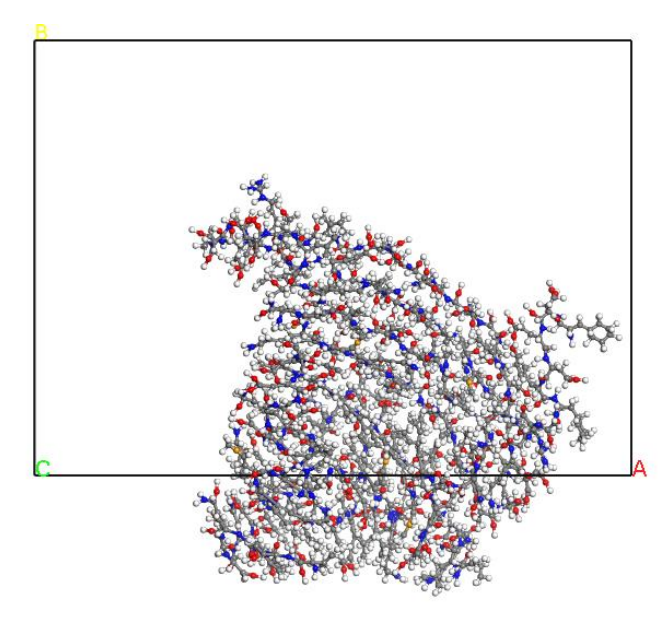


Figure 10 Structural model of the SF

## 2.2 Model optimization

The blend model for sil-ma, HA and  $\beta$  -tcp was optimized under the Dreiding force field with the number of iterations set to 600000. Then the annealing simulation was conducted at 300 K, the NPT ensemble (that is, the setting conditions of the number of atoms, pressure and temperature), the number of cycles was 5, the total number of steps is 50000, a total duration of 500ps, one conformation per 1000 steps, and the structure of the resulting model was optimized as shown in Figure 11.

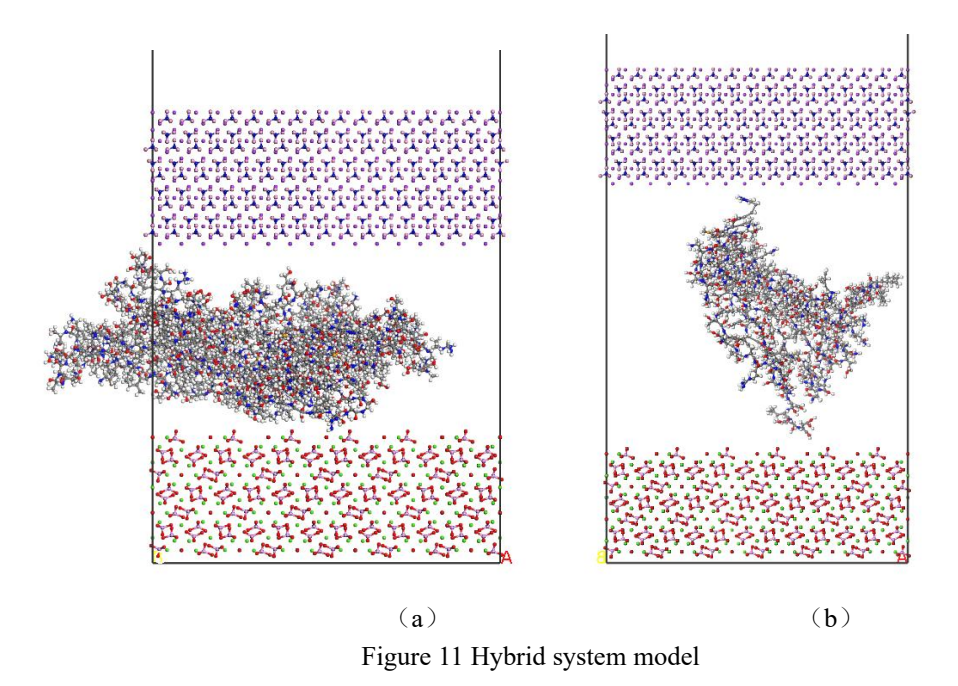


Figure 11a shows the blend model for sil-ma and HA and  $\beta$ -tcp, and b shows the blend model for SF and HA and  $\beta$ -tcp

## 3 Results and Discussion

## 3.1 Radial distribution function

The radial distribution function g(r) is the characteristic physical quantity reflecting the microstructure of the material, representing the ratio of the probability density of another molecule at a distance of r relative to the randomly distributed probability density. The radial distribution function g(r) analysis of the entire equilibrium trajectory can reveal the way and nature of the material interaction.

The atomic types in the molecular chain of Sil-ma hydrogel include main chain C atom, hydroxyl O atom, hydroxyl group

H atom and H atom connected to main chain C, surrounded by H atoms and amino group, which is difficult to interact with HA. Therefore, we only consider the remaining three types of atoms and record them as O 1 and H1 in turn. Similarly, the atomic types in HA molecules are C, H, O, P, Ca atoms, which P atoms by 3 O atoms isolation, so only consider Ca, H and O, the three types of atoms as HA-O, HA-H, here the g between oxygen and oxygen atoms, oxygen and hydrogen interaction  $g(r) \sim r$  relationship is analyzed, as shown in Figure 12.

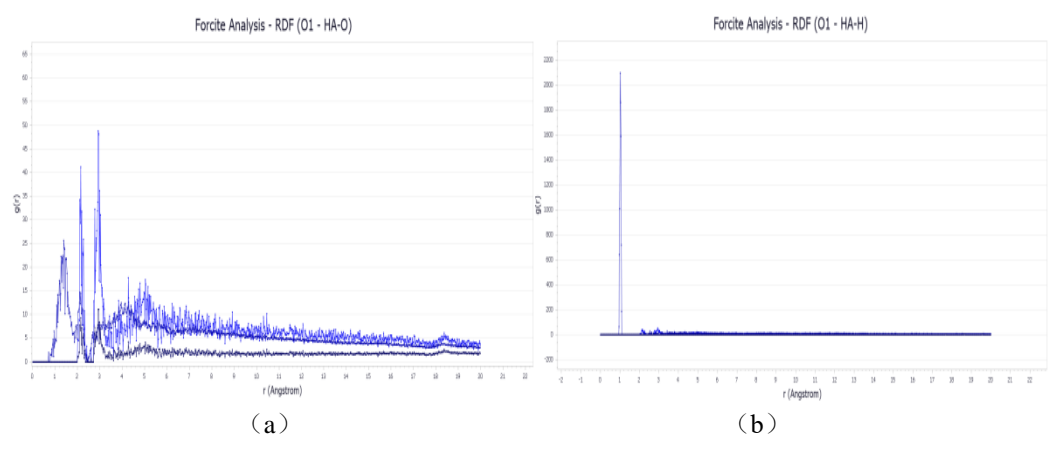


Figure 12 Radial distribution function plot

Figure 12a shows the radial distribution function of Sil-MA oxygen atoms and HA oxygen atoms in the hybrid system, and b is the radial distribution function between Sil-MA oxygen atoms and HA hydrogen atoms in the hybrid system

The intermolecular radial distribution function can reveal the interaction mode and essence of non-bonded atoms. Generally speaking, the peaks within 0.35 nm in the radial distribution function diagram are mainly composed of chemical bonds and hydrogen bonds, while the  $0.35 \sim 0.50$  nm are mainly van der Waals (vdw) force components. The radial distribution function of O 1-Ob in Figure (a) achieves a peak near r=0 nm, Mainly because of the strong covalent bonding interaction between O1 and HA-O, Thus draws the distance between O 1 and HA-O; the radial distribution function of O1-HA-H in Figure (b) obtains the first peak near r=0.1nm, This is the hydrogen bond formed between the O atom and the H atom in the sil-ma; The radial distribution function analysis showed that, The interaction between sil-ma and HA is mainly through the formation of covalent bonds with O in the sil-ma and O in the sil-ma molecular unit, O in the sil-ma molecular unit forms an oxygen-hydrogen bond with H in HA, Bond formation indicates that a chemical crosslinking of the material occurs, The material with a more stable nature, The mechanical strength further reveals the nature of the chemical bond between the two materials.

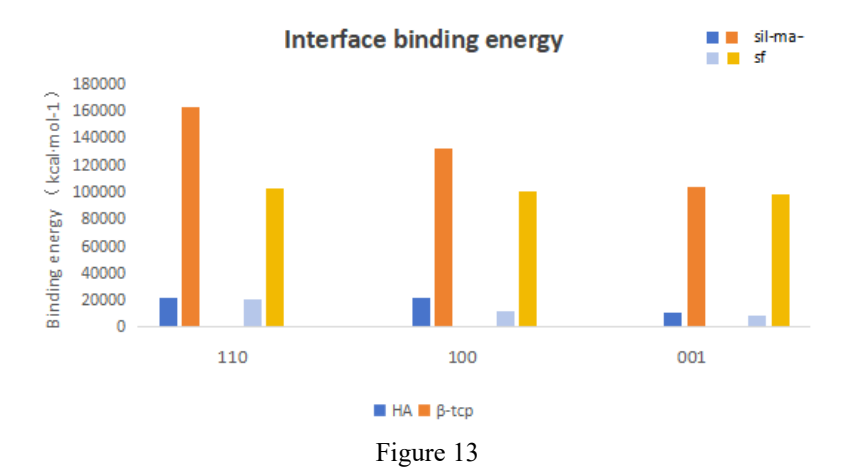
#### 2.2 Interface binding energy

The adhesion between HA,  $\beta$  -tcp and organic polymer materials can be evaluated by the interfacial binding energy between HA,  $\beta$  -tcp crystal surfaces and organic polymer materials, so as to analyze the microscopic factors of the changes in the mechanical properties of the materials.

Calculated by the following formula [17]:

$$E_{\rm binding} = E_{\rm HA/\beta\text{-}tcp\,surface} + E_{\rm poly\,mer} \text{--} E_{\rm HA/\beta\text{-}tcp\,+poly\,mer}$$

among  $E_{\text{HA/\beta-tcp}}$ Is the energy of the HA /  $\beta$  -tcp surface, and the  $E_{\text{polymer}}$   $E_{\text{HA/\beta-tcp+polymer}}$ Is the energy of the protein molecular chain, is the energy of the HA or  $\beta$  -tcp surface with the protein molecule, and M is the number of atoms in each molecular chain. Note that the high binding energy indicates a high bond strength between the polymer material and the HA /  $\beta$  -tcp surface.



Through the comparative analysis of the interface binding energy of SF and Sil-MA hybrid systems, we found that the interface binding energy of Sil-MA with HA and  $\beta$  -tcp is much higher than that of SF hybrid system, indicating that the stability of Sil-MA hybrid system is higher than that of SF hybrid system. In the study, through the analysis of the three surfaces of HA and  $\beta$  -tcp crystals, we found that the highest binding energy in the 110 plane, which is in line with the conclusion of other researchers and further verified the correctness of the study model (See Figure 13).

## 3 Mechanical performance evaluation

#### 3.1 Preparation of the Sil-ma

40g of silkworm cocoons were boiled in 1 L of 0.05 M anhydrous sodium carbonate solution for 30 min at 100°C to remove sericin, and then washed several times with distilled water. Subsequently, the unglued silk was dried at room temperature and 20g of it was dissolved in 100 mL of 9.3M lithium bromide (LiBr) solution at 60°C for 1 hour. Immediately after dissolving SF with LiBr, 4 mL of glycidyl methacrylate (GMA) solution (Sigma-Aldrich, St. Louis, USA) was added to the mixture and stirred at 300rpm for 3 h at 60°C. Then, the resulting solution was dialyzed against distilled water for 4 days using a dialysis bag. Finally, the solution was frozen in-80°C for 12 hours and freeze-dried for 48 hours. The lyophilized Sil-MA powder was stored at-80°C for further use.

#### 3.2Preparation of SF

40g of silkworm cocoons were boiled in 1 L of 0.05 M anhydrous sodium carbonate solution for 30 min at  $100^{\circ}$ C to remove sericin, and then washed several times with distilled water. Subsequently, the unglued silk was dried at room temperature and 20g of it was dissolved in 100 mL of 9.3M lithium bromide (LiBr) solution at  $60^{\circ}$ C for 1 hour. Cooling to room temperature, and centrifuged at 9.000 r / min for 10 min. The centrifugal filin protein solution was transferred to a dialysis bag for 4 days. Finally, the dialysis bag containing filin protein solution was concentrated in a polyethylene glycol solution with 10% mass fraction for 12 h and stored in a  $4^{\circ}$ C refrigerator.

### 3.3 Fourier infrared spectrum

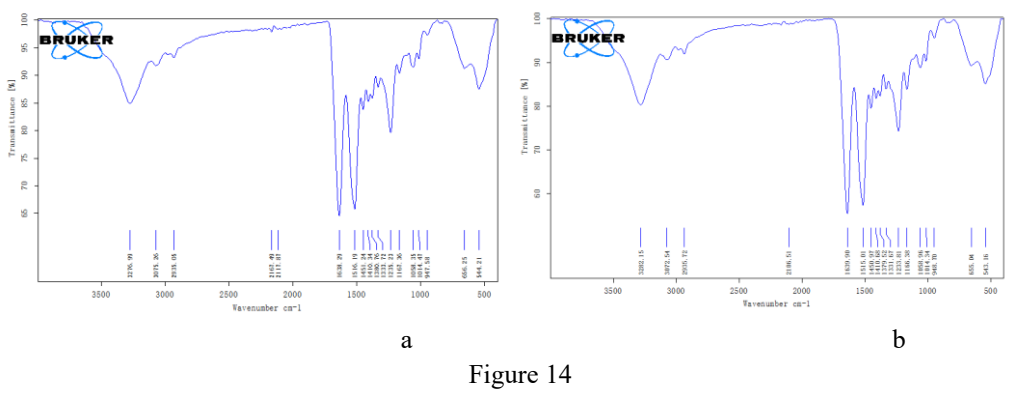
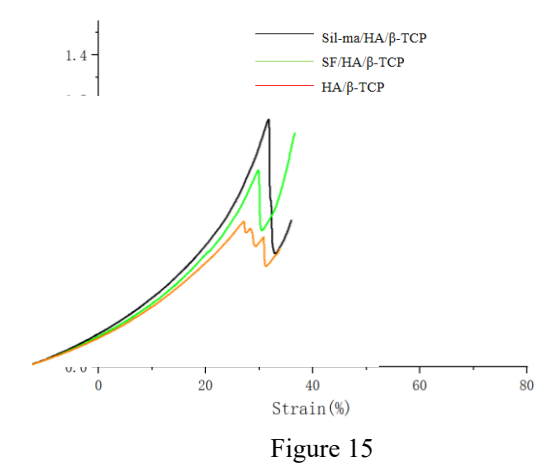


Figure 14a shows the SF IR spectrum, and b shows the Sil-MA IR spectrum

Comparison of infrared spectra of both SF and sil-ma reveals the characteristic peak of SF amide I band 1638cm-1, while at 1238cm 1, a weak band is visible for the Sil-ma group, indicating the CHOH stretching of the alcohol group produced after ring opening of the GMA epoxy group. Therefore, sil-ma is modified to SF; the characteristic peak of peak of Sil-MA amide I band 1638cm-1 is higher than that of SF, which indicates that the content of secondary conformation  $\beta$  -folded structure in sil-ma is slightly enhanced, which is most likely due to the higher mechanical performance of sil-ma than sf (See Figure 14). 3.4 Compression test

For macromechanical observation of the SF / Sil-MA hydrogel mixed precursor ceramic material, a cylindrical sample was prepared by loading the hydrogel composite into a custom PDMS mold (8 mm high; 10 mm diameter) and then 1min under UV (435n m). Using Instron 5566, the tester performs the compression test at a load rate of 1 mm / min for [18] and a 50 N weighing cell, see Figure 15.



Testing of mechanical properties of hydrogel composites of SF and Sil-MA systems shows that the compression resistance of Sil-MA composite systems is higher than that of SF composite systems, and this may be due to the mechanical properties of SF depending on the  $\beta$  in SF, which is lower than the  $\beta$  in Sil-MA, and thus macroscopically lower mechanical properties than Sil-MA.

## 4 Conclusion

In this study, molecular dynamics simulations of SF, Sil-MA, HA, and  $\beta$  -tcp composite models and experimental validation draw the following conclusions:

- (1) The radial distribution function shows that the interaction mode of sil-ma with HA and  $\beta$ -tcp is mainly through O bonding between O and HA and  $\beta$ -tcp in sil-ma molecular unit, and O and H in HA in sil-ma molecular unit. The electrostatic power binds the material better, revealing the nature of chemical cross-linking between materials and enhancing the mechanical properties of materials.
- (2) From the molecular level analysis, it is found that the interface binding energy of Sil-MA material and precursor ceramic mixture is higher than that of SF material, which reflects the stability of Sil-MA material system from the microscopic point of view, and provides the microscopic theoretical basis for the macroscopic mechanical behavior of the material.
- (3) The mechanical performance of Sil-MA system is higher than SF, on the one hand is a verification of the theoretical analysis, and on the other hand, shows the correctness of choosing Sil-MA as the matrix material in this study.

## **Declaration of Conflicting Interests**

The author(s) declared no potential conflicts of interest with respect to the research, author-ship, and/or publication of this article.

## **Data Sharing Agreement**

The datasets used and/or analyzed during the current study are available from the corresponding author on reasonable request.

## **Funding**

The author(s) received no financial support for the research, authorship, and/or publication of this article.

#### References

- [1] Kim, S.H., Yeon, Y.K., Lee, J.M.et al. Precisely printable and biocompatible silk fibroin bioink for digital light processing 3D printing. Nat Commun 9, 1620 (2018).
- [2] Kitsugi, T., et al., Transmission electron microscopy observations at the interface of bone and four types of calcium phosphate ceramics with different calcium/phosphorus molar ratios. Biomaterials, 1995. 16(14): p.1101-7.
- [3] Wu X , Zhou M , Jiang F ,et al.Marginal sealing around integral bilayer scaffolds for repairing osteochondral defects based on photocurable silk hydrogels ScienceDirect[J].Bioactive Materials, 2021, 6(11):3976-3986.DOI:10.1016/j.bioactmat.2021.04.005.
- [4] Einhorn, T.A.and L.C.Gerstenfeld, Fracture healing: mechanisms and interventions.Nat Rev Rheumatol, 2015. 11(1): p.45-54.
- [5] HUANG YLU D B,ANGUILANO L.at al Fatbication and characterization of a biodegradable Mg-2Zn-0.5Ca/18-TCP composite(J Materials Science and Engineering C,2015,54:120-132.
- [6] HE s Y.SUNY OHEN MfF t al Microstructure and properties of iodegradable p-TCP reinforced Mg-Zn-Zr composites[IJ Transactions of Nonferrous Metals Society of China, 2011, 21(4):814-819.
- [7] Wang Jian, Ma Xiangyu, Feng Yafei, etc. Promotion of magnesium ions on osteoblast viability and differentiation and its mechanism [J]. Modern biomedical advances, and 2015,15(15):2836-2839.DOI:10.13241/j.cnki.pmb.2015.15.009.
- [8] Liu J, Li L, Suo H, et al.3D printing of biomimetic multi-layered GelMA/nHA sc affold for osteochondral defect repair [J].Materials & Design, 2019, 171: 107708.
- [9] Sun H. Compass: An ab intio force-field optimized for con-densedphase application-Overview with details on alkane and benzene compounds [J]. J Phys Chem B, 1998, 102(38): 7338-7364.
- [10] D.Sun, J.ZhouEffect of water content on microstructures and oxygen permeation in PSiMA-IPN-PMPC hydrogel: a molecular simulation study Chem.Eng.Sci., 78 (2012), pp.236-245.
- [11] M.Yuan, W.Nie, H.Yu, et al. Experimental and molecular dynamics simulation study of the effect of different surfactants on the wettability of low-rank coal J.Environ. Chem. Eng., 9 (5) (2021)
- [12] O.Bertran, C.Saldías, D.D.Díaz, et al.Molecular dynamics simulations on self-healing behavior of ionene polymer-based nanostructured hydrogels Polymer, 211 (2020)
- [13] X.Tan, Z.Xue, H.Zhu, X.Wang, D.XuHow Charged Amino Acids Regulate Nucleation of Biomimetic Hydroxyapatite Nanoparticles on the Surface of Collagen Mimetic Peptides: Molecular Dynamics and Free Energy Investigations Cryst.Growth Des., 20 (2020), pp.4561-4572,
- [14] Wu Jialong. mechanics of elasticity [M]. Shanghai: Tongji University Press, 1993.
- [15] Swenson RJ. Comments on virial theorems for bounded systems [J]. Am J Phys, 1983, 51(10): 940-942.
- [16] Watt JP, Davies GF, O'Connell RJ. The elastic properties of composite materials [J]. Rev Geophys Space Phys, 1976, 14(4): 541-563.
- [17] JANDREA P, SIMONE T, GIOVANNI G,et al Mechanical and thermal properies of graphene random nanofoams via molecular dynamios simulations. J. Ccarbon, 2015, 132:766-775.
- [18] PETTIFOR D,MATER G.Theoretical predictions of structure and related properties of intermetallics[J].Sci.Technol.,1992,8:345.

Vol: 2025 | Iss: 1 | 2025 | © 2025 Fuel Cells Bulletin